Galaxies, Cosmology and Dark Matter

Lecture given by
Ralf Bender
USM

Script by:
Christine Botzler, Armin Gabasch,
Georg Feulner, Jan Snigula

Summer semester 2000

Chapter 5

Spiral Galaxies

5.1 Components of Spiral Galaxies

Disk: metal rich stars, strong rotation, star formation, HI, H_2-gas, molecular clouds, dust, hot gas (heating by star formation and supernovae)

Bulge: metal poor to super metal rich stars, weak rotation, concentrated in the central part, (barrish?)

Stellar halo: metal poor stars, little/no rotation, wide variety of orbits, globular clusters, X-ray gas, low density HI/HII-gas

Dark halo: dominating mass outside of 10 kpc, (maybe) slightly flattened

5.2 Radial Brightness and Density Profiles

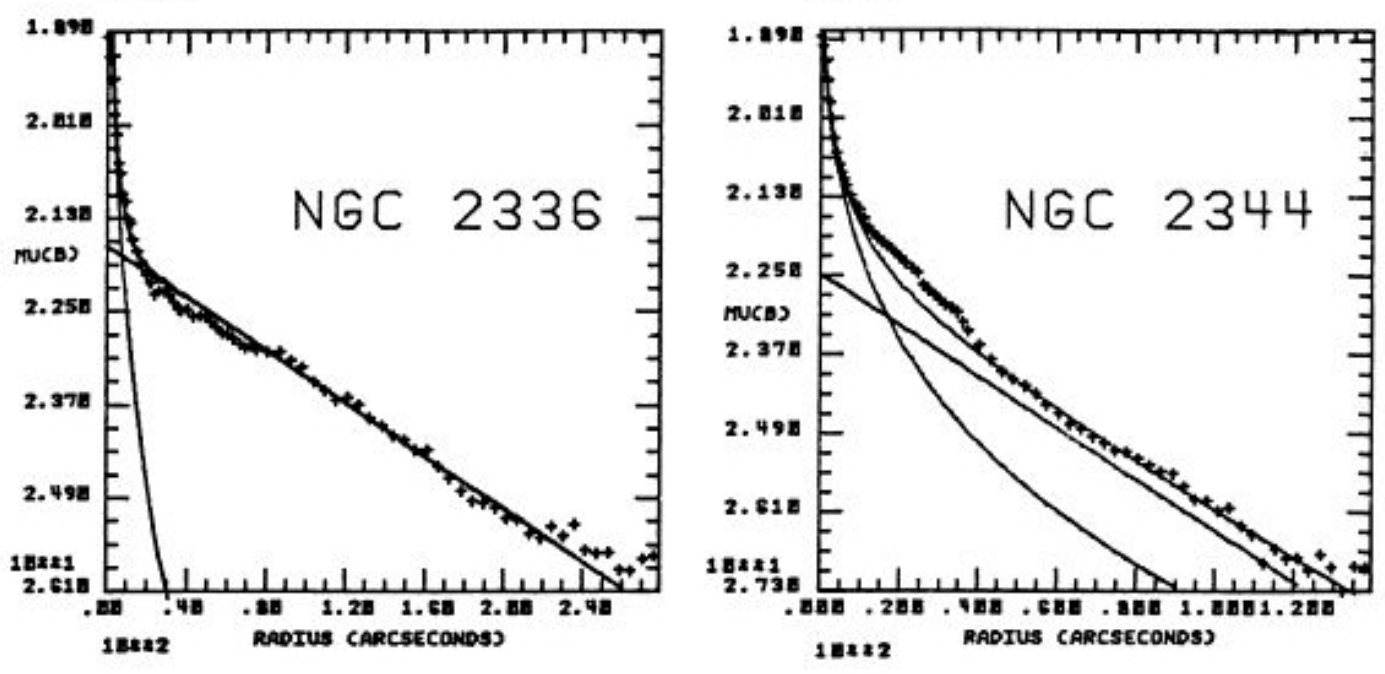

FIG. 6.—Elliptically averaged profiles for the 26 spiral galaxies. For NGC 4594 the north half of the minor axis is shown. Where an iterative decomposition was possible, disk, bulge, and total profiles are shown. In all other cases, only the bulge fit is shown.

see: T. Boroson (1981) *ApJS*, **46**, 177

Surface Brightness Distribution:

Bulges: typically de Vaucouleurs or $r^{\frac{1}{4}}$-profile

$$\boxed{\Sigma(r) = \Sigma_e \cdot 10^{-3.3307\left(\left(\frac{r}{r_e}\right)^{\frac{1}{4}}-1\right)}} \quad \Sigma: \text{ surface brightness}$$

$$L_{tot} = 7.215 \cdot \Sigma_e \cdot \pi r_e^2$$

$$\left.\begin{array}{l}\text{projected}\\ \text{luminosity}\\ \text{within } r_e\end{array}\right\} L(r_e) = \frac{L_{tot}}{2} \rightarrow r_e = \text{half-light radius}$$

$$\begin{aligned}\text{Units:} \quad [\Sigma] &= \frac{L_\odot}{pc^2}\\ [SB_\alpha] &= [\mu_\alpha]\\ &= [-2.5\log\Sigma + 21.55 + M_{\odot,\alpha}]\\ &= \frac{\text{mag}}{\text{arcsec}^2}\end{aligned}$$

Disks: typically exponential profile, $R_0 =$ scale length

$$\boxed{\Sigma(r) = \Sigma_0 e^{-\frac{r}{R_0}}}$$

$$L_{tot} = 2\pi\Sigma_0 R_0^2$$

Density distribution:

Stellar halo: existence confirmed only in the Milky Way $(\mu \gtrsim 26 \frac{\mathrm{mag}}{\mathrm{arcsec}^2})$
$\rho_H \sim r^{-3.5}$, $\rho_H(R_\odot) \simeq \frac{\rho_{\mathrm{disk}}}{1000}$

Globular clusters: $n_{\mathrm{gc}} \sim r^{-3.5}$, $n_{\mathrm{gc}}(10\mathrm{kpc}) \simeq 10^{-3} kpc^{-3}$ (in the Milky Way)

Dark Matter Halo: $\rho_{\mathrm{DM}} \sim r^{-2}$, $r < 100...200\,$kpc

5.3 Characteristic Parameters of Bulges and Disks

	M31	Galaxy
Bulge		
Luminosity ($L_{B,\odot}$)	7.7×10^9	2×10^9
Luminosity (fraction of total)	0.25	0.12
Effective radius (kpc)	2.2	2.7
Axis ratio	0.57	0.85
Velocity dispersion ($km\,s^{-1}$)	155	130
Number of globular clusters	$400 - 500$	$160 - 200$
Disk		
Luminosity ($L_{B,\odot}$)	2.4×10^{10}	1.7×10^{10}
Central surface brightness ($\frac{L_{B,\odot}}{pc^2}$)	~ 95	~ 110
Scale length (kpc)	6.4	5.0
B - V (errors about 0.1)	0.76	0.85
HI gas content ($M_\odot$)	3×10^9	4×10^9
Rotation velocity ($km\,s^{-1}$)	260	220
IRAS infrared luminosity ($L_\odot$)	2.6×10^9	1.5×10^{10}
Gas metallicity gradient ($dex\,kpc^{-1}$)	-0.04	-0.08

5.4 Globular Cluster Systems of Galaxies

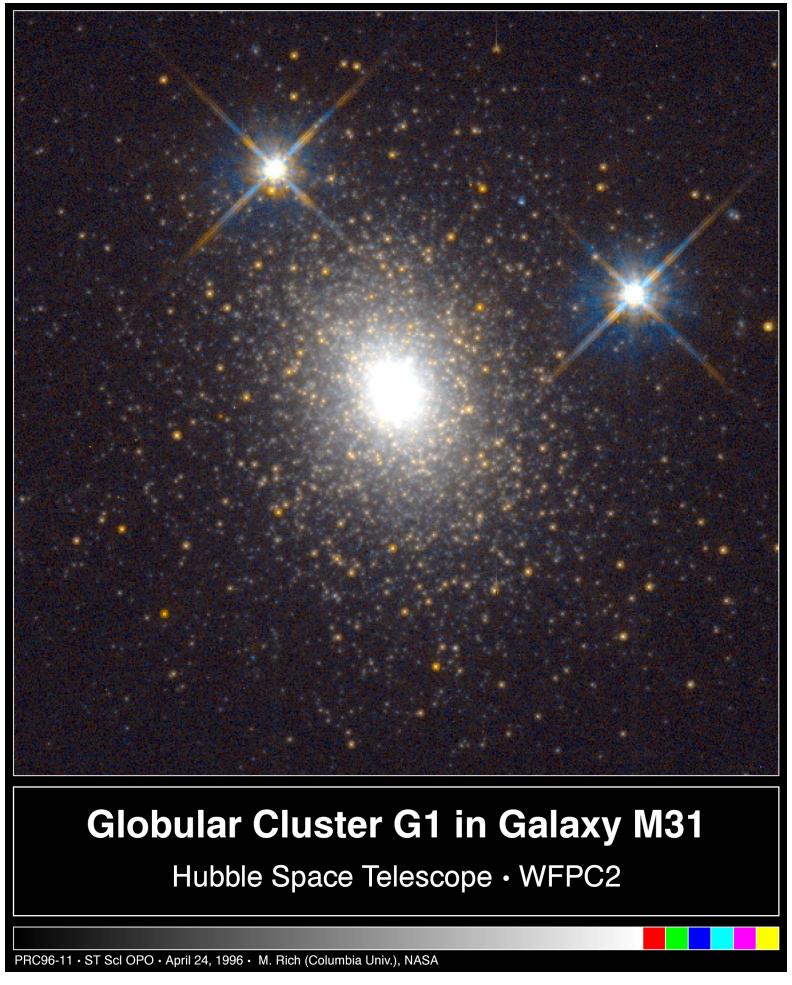

Besides disk and bulge, the globular cluster systems and the halo stars are other important components of spirals. Compared to disks and bulges these components are by a factor of 10 . . . 1000 more metal poor. Typical ages for globular clusters in the Milky Way are 12 Gyr to 15 Gyr. Therefore, globular clusters and halo stars seem to be the oldest objects in spirals (consistent with their metallicity).

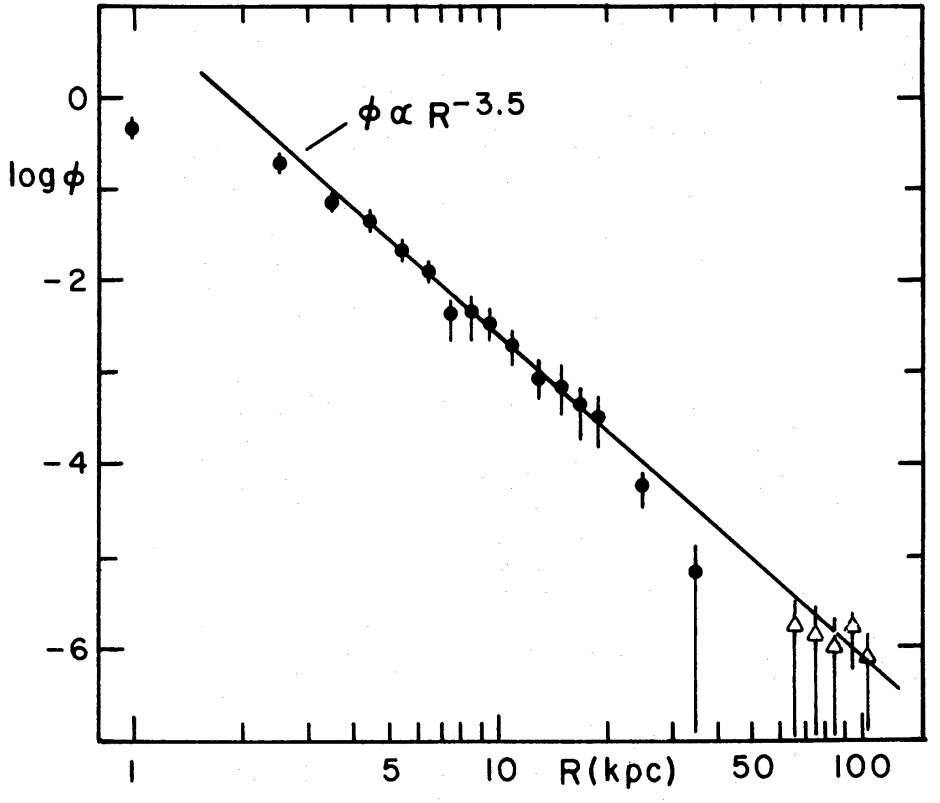

FIG. 2.—The number of clusters per cubic kiloparsec (ϕ) is plotted against galactocentric distance (R). The solid circles represent the clusters with $|Z| < 20$ kpc; the open triangles represent the clusters with $|Z| > 37$ kpc. There are no clusters in the zone $33 < R < 60$ kpc.

see: Zinn (1985)

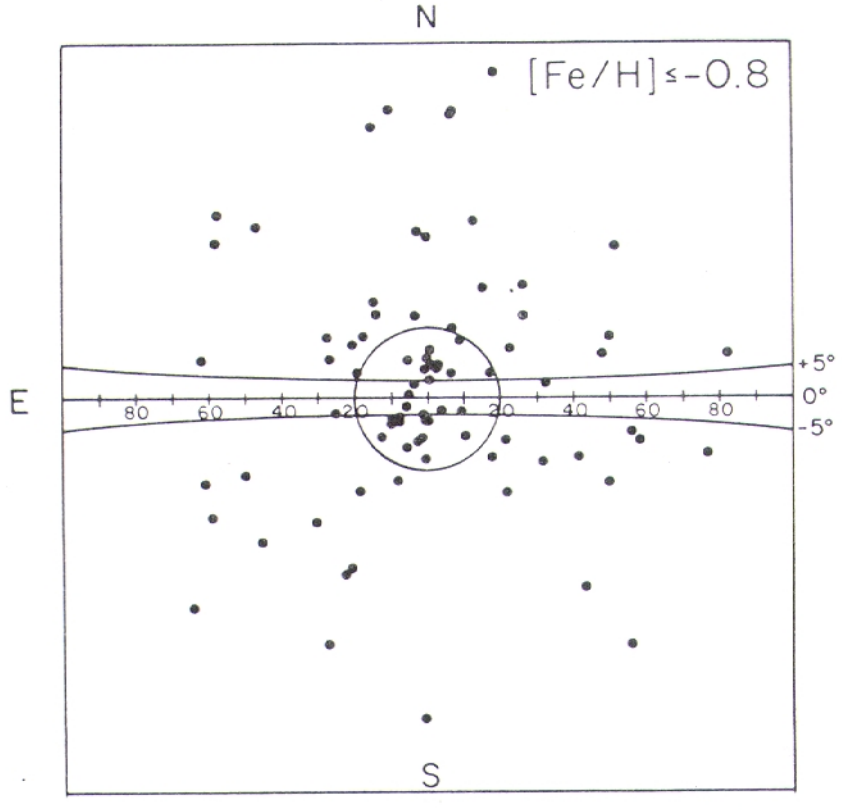

see: Gilmore, King, van der Kruit (1989)
Saas Fee Course

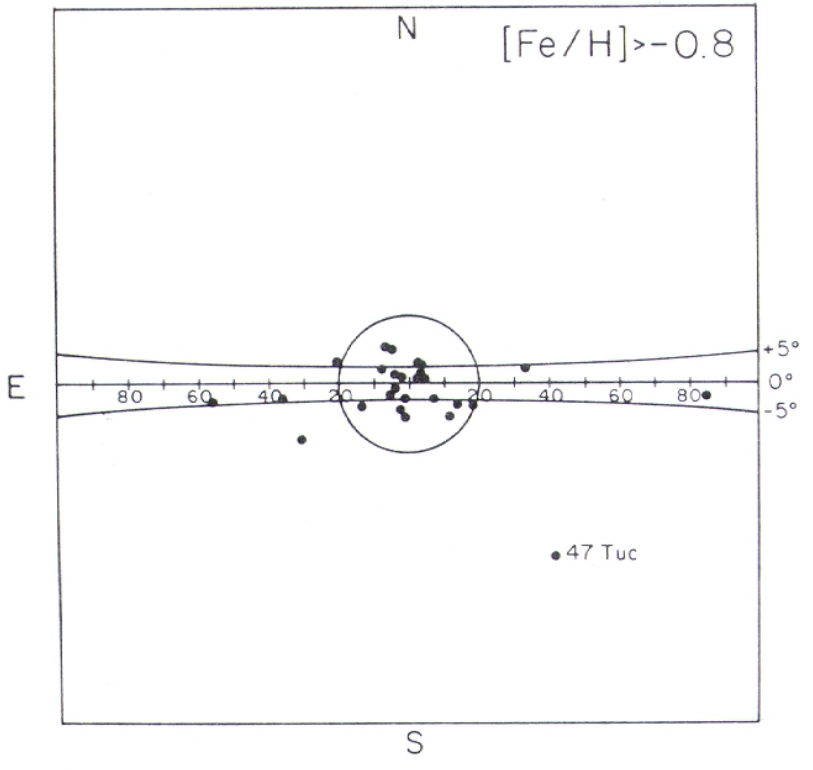

FIGURE 3.11
Comparison of the distributions on the sky of weak-lined (above) and strong-lined (below) globular clusters. (From Zinn 1985.)

5.5 Star Formation History in Spirals

- **The H_α-line strength and the far-infrared luminosity provide information about the present star formation rate Ψ in galaxies.** The H_α strength is directly proportional to the ionizing flux of massive, hot stars and thus to the number of these stars that is a measure of the actual star formation rate. The far-IR-luminosity comes from warm dust grains which are surrounding the star formation regions. These grains absorb a large fraction of the UV photons, heat up and radiate blackbody radiation at their equilibrium temperature.

- **Colours and H_α-equivalent widths provide information about the star formation history.** A high star formation rate in the past will have produced many low-mass red stars that cause the galaxy to appear redder and to have more continuum light. The H_α-equivalent width (a measure for the strength of the H_α emission relative to the underlying continuum) is an indicator of how many stars are currently formed relative to the average star formation rate over the history of the galaxy.

- Comparing the H_α-flux with colours leads to:

$$\frac{\text{present } \Psi}{\langle \Psi \rangle} = \begin{cases} < 1 & \text{for Sa...Sb} \\ \simeq 1 & \text{for Sc} \\ > 1 & \text{for Sd...Im} \end{cases}$$

  (for a schematic star formation history of different Hubble types see Sandage (1996))

- The relation between the equivalent width of H_α compared to a colour (e.g. B-V) is an indicator for the slope of the initial mass function (IMF). Current data show compatibility with the Salpeter IMF and are probably incompatible with a Miller-Scalo IMF.

Equivalent width (EW):

This is the width of a section of the continuum near the line which contains as much light as is either contributed by the line (for an emission line) or blocked by the line (for an absorption line).

$$EW = \frac{\int f_{\lambda,line}\, d\lambda}{f_{\lambda,continuum}}$$

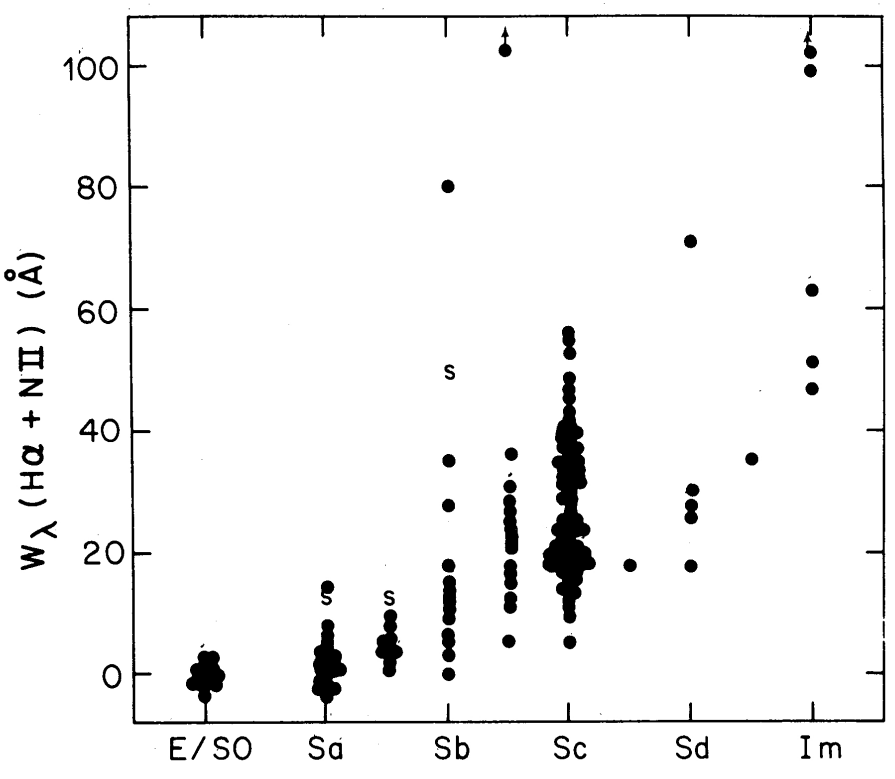

FIG. 5. Distribution of Hα + [N II] emission equivalent width, binned by RSA Hubble type. The symbol *S* denotes a Seyfert galaxy.

see: Kennicutt et al. (1983) *AJ*, **88**, 1098

A SURVEY OF Hα EMISSION IN NORMAL GALAXIES

ROBERT C. KENNICUTT, JR.
Department of Astronomy, University of Minnesota, Minneapolis, Minnesota 55455

STEPHEN M. KENT
Department of Astronomy, California Institute of Technology, Pasadena, California 91125
and Center for Space Research, Department of Physics, Massachusetts Institute of Technology, Cambridge, Massachusetts 02139[a)]
Received 28 January 1983; revised 29 April 1983

ABSTRACT

We present the combined results of photometric and spectrophotometric surveys of Hα emission in 200 field and Virgo cluster galaxies. In most spiral galaxies the emission is dominated by normal disk H II regions, and consequently the integrated Balmer flux of a galaxy can be used as a quantitative index of its current OB star formation rate. Uncertainties due to instrumental effects, nuclear emission, [N II] emission, and extinction by dust are evaluated. The integrated emission of a galaxy is strongly correlated with its Hubble type and color, confirming the earlier conclusions of Cohen. Emission among galaxies of a given type varies greatly, however, and in most cases is due to a real dispersion in star formation activity. This activity is only weakly correlated with galaxy luminosity or H I content, suggesting that some other parameter is more important.

see: Kennicutt et al. (1983) *AJ*, **88**, 1098

150	Sbc	21.3	24 ± 2	41.77:	5.1:
278	Sbc	20.7	36 ± 2	41.76	4.9
3310	Sbc	20.8	113 ± 4	42.15	12.2
4666	Sbc	21.5	31 ± 2	42.04	9.7
5033	Sbc	21.1	17 ± 2	41.60:	3.5:
5055	Sbc	21.3	15 ± 1	41.65:	3.8:
5194	Sbc	21.6	24 ± 2	41.95:	7.6:
5248	Sbc	21.2	21 ± 1	41.71:	4.3:
5970	SBbc	21.4	24 ± 5	42.15	12.4
6217	SBbc	21.1	29 ± 2	41.81	5.4
6574	Sbc	21.3	27 ± 5	41.94	7.6
7392	Sbc	21.7	11 ± 4	41.85	6.2
7479	SBbc	22.3	12 ± 3	41.98:	8.1:
157	Sc	22.2	28 ± 2	42.18	13.2
337	Sc(p)	21.1	49 ± 4	41.97	8.1
428	Sc	20.6	18 ± 3	41.38	2.0
450	Sc	20.7	38 ± 4	41.68	4.1
628	Sc	21.8	24 ± 2	41.99	8.4
672	SBc	19.9	20 ± 3	41.06	1.0
949	Sc	19.8	21 ± 3	41.04	1.0
1058	Sc	19.3	21 ± 3	40.86	0.6
1073	SBc	20.9	20 ± 3	41.49	2.7
1084	Sc	21.6	41 ± 2	42.15	12.1
1087	Sc	21.4	35 ± 3	41.97	8.1
1232	Sc	22.6	20 ± 3	42.32:	17.8:
1385	Sc	21.8	46 ± 2	42.21	14.0
1518	Sc	19.4	33 ± 4	41.15	1.2
1637	Sc	19.7	16 ± 2	41.02	0.9
2139	SBc	21.2	46 ± 3	41.91	7.0
2276	Sc	22.1	42 ± 4	42.35	19.4
2763	Sc	20.5	29 ± 2	41.53	3.0
3389	Sc	19.9	35 ± 4	41.32	1.8
3486	Sc	20.1	35 ± 4	41.41	2.2
3631	Sc	21.3	30 ± 3	41.87	6.5

see: Kennicutt et al. (1983) *ApJ*, **272**, 54

SFR Ψ:

$$\frac{\Psi}{M_\odot/yr} \simeq \frac{L_{H_\alpha}}{10^{41} erg/sec}$$

underlying assumption is the so-called case B approximation:

Photons of the Lyman-continuum are completely absorbed and reemitted as Ly_α, H_α, etc. (see Osterbrock: *Astrophysics of Gaseous Nebulae*)

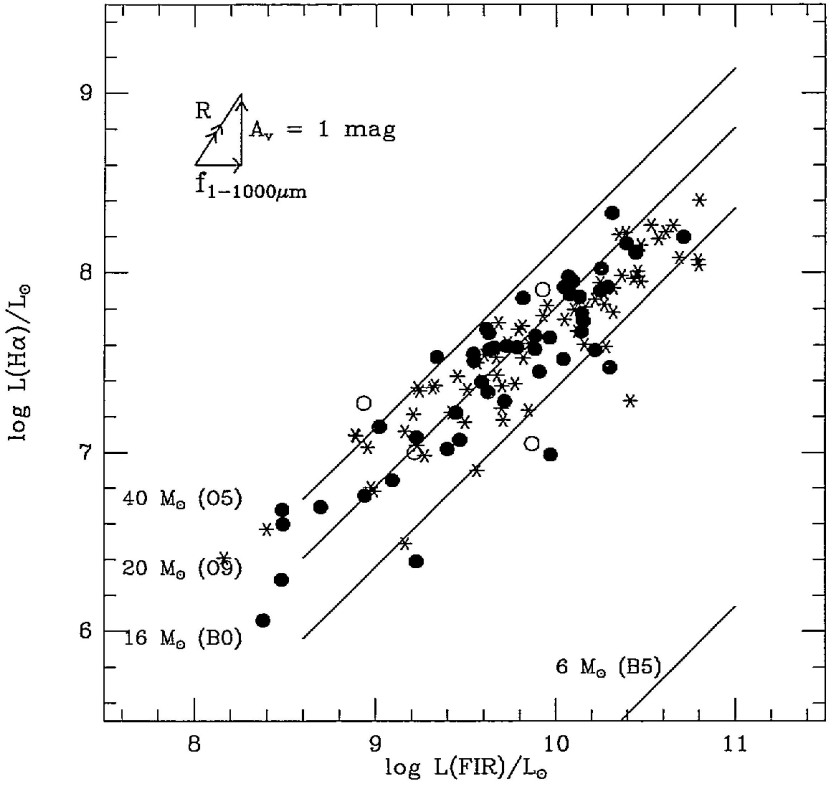

FIG. 1.—The correlation between the Hα emission line and the *IRAS* 40–120 μm luminosity for spiral galaxies. The points are coded by $S_{100\,\mu m}/S_{60\,\mu m}$ color; stars identify spirals with $S_{100\,\mu m}/S_{60\,\mu m} \leq 2.5$, filled circles identify spirals with $2.5 < S_{100\,\mu m}/S_{60\,\mu m} \leq 3.5$, and open circles identify spirals with $S_{100\,\mu m}/S_{60\,\mu m} > 3.5$. The lines show the ratio $L_{H\alpha}/L_{bol}$ expected for an H II region powered by stars of masses 40, 20, 16, and 6 $M_\odot$, respectively. Extrapolating the *IRAS* 40–120 μm luminosity to 1000 μm and correcting the observed Hα emission line luminosity by 1 mag of extinction translates the data points by an amount equivalent to that illustrated by the vector ***R***. The fact that the data points lie between the solid lines illustrates that the observed far-infrared luminosity is equivalent to the luminosity which is expected from the massive stars that are required to ionize the hydrogen gas.

see: Devereux et al. (1990) *ApJ*, **350**, 25

THE ORIGIN OF THE FAR-INFRARED LUMINOSITY FROM SPIRAL GALAXIES

NICHOLAS A. DEVEREUX AND JUDITH S. YOUNG
Department of Physics and Astronomy, University of Massachusetts; and The Five College Radio Astronomy Observatory
Received 1989 October 10; accepted 1989 November 28

ABSTRACT

The relationship between the far-infrared and Hα luminosity has been investigated for a sample of 124 spiral galaxies. After correcting the Hα luminosities for an average 1 mag of extinction and extrapolating the *IRAS* 40–120 μm luminosity to 1000 μm, we find that the mean ratio of Hα to far-infrared luminosity is comparable to that expected from H II regions powered by stars with masses $>6\,M_\odot$. This result constitutes strong evidence in support of the view that high-mass ($>6\,M_\odot$) O and B stars are responsible for *both* the Hα and far-infrared emission in spiral galaxies of high, $\geq 1 \times 10^9\,L_\odot$, far-infrared luminosity.

Subject headings: galaxies: stellar content — infrared: general

see: Devereux et al. (1990) *ApJ*, **350**, 25

O/B stars → photons of the Lyman continuum

↗ ionisation of the gas → Ly_α, H_α, etc. photons

↘ heating of the dust to 10...1000 K → thermal far-IR emission

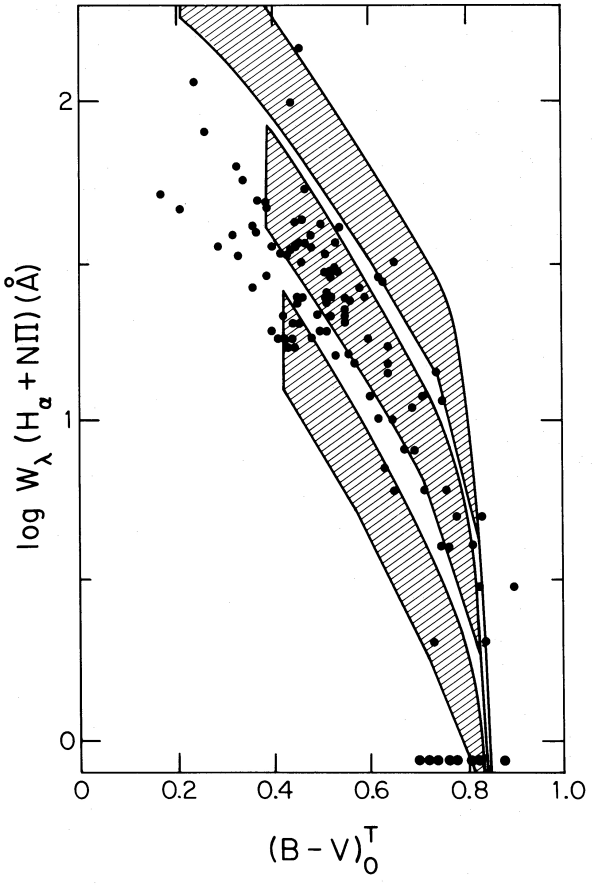

FIG. 4.—Observed emission line equivalent widths and corrected RC2 colors for observed galaxies, along with the evolutionary models. The effect of dust has been shown by plotting each model as an area, as described in the text. The IMFs corresponding to each model are the same as in Fig. 3.

see: Kennicutt et al. (1983)
ApJ, **272**, 54

The three evolutionary models use different IMF (from top to bottom):

$\Phi \sim m^{-2}$

$\Phi \sim m^{-2.35}$

$\Phi \sim$ Miller-Scalo IMF

$$W_\lambda \simeq \frac{H_\alpha \text{ flux}}{\text{continuum flux}} \simeq \frac{\text{present SFR}}{\text{luminosity of old stars}}$$

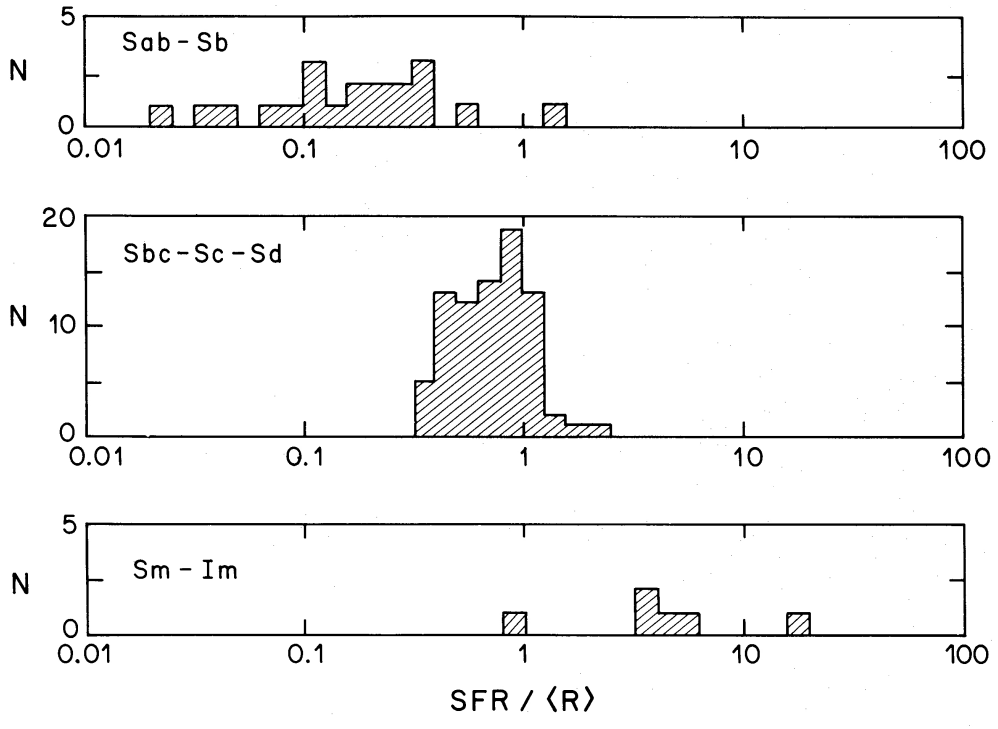

FIG. 6.—Distribution of current star formation rates, normalized to the average past rate in each galaxy. The small Sab–Sb and Sm–Im samples may be somewhat biased. The irregular galaxy sample is certainly biased toward active (bursting) star forming systems.

see: Kennicutt et al. (1983) *ApJ*, **272**, 54

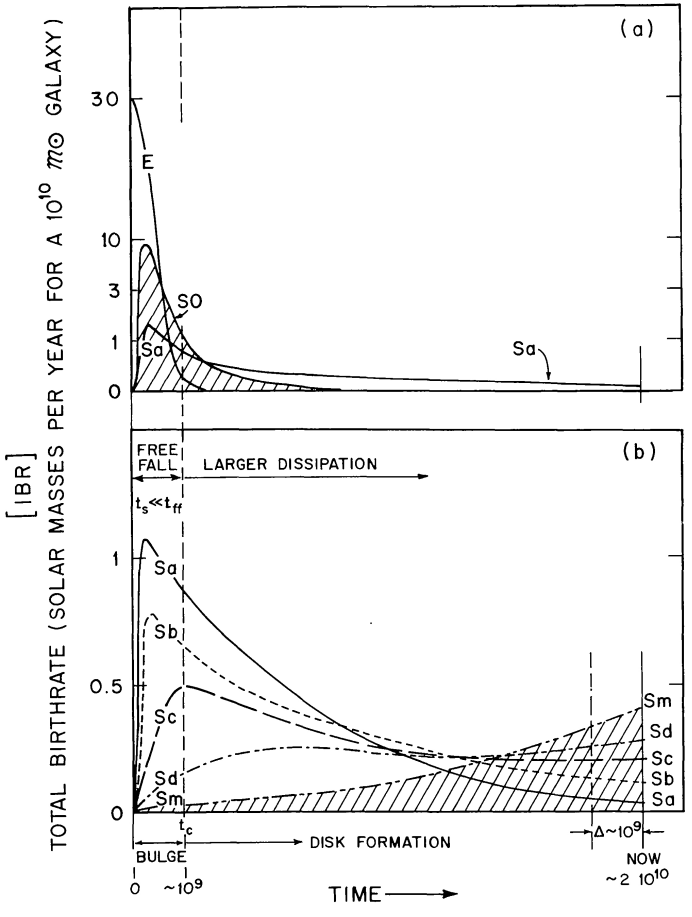

Fig. 10. Same as Fig. 9 with later Hubble types shown in the lower panel. The integral under the Sm curve is shaded for illustration. The curves are only schematic showing the trends that have been established by Gallagher et al. (1984)

see: Sandage et al. (1989) *A&A*, **161**, 89
very schematic

5.6 Stellar Population of the Galactic Bulge

- Stars of the bulge are old low mass stars with ages of 5...12 Gyr (as observed in 'Baade's window')
- The metallicity distribution ist consistent with a **closed-box-model**, which can be derived as follows:
  The mass of the not yet processed gas as a function of its metallicity is:

$$M_g(Z) = M_{g,0} \exp\left(-\frac{Z}{y}\right)$$

  which has the derivative:

$$dM_g(Z) = -\frac{M_{g,0}}{y} \exp\left(-\frac{Z}{y}\right) dZ$$

  $dM_g(Z)$ is the fraction of mass with a metallicity in the interval [Z, $Z + dZ$].
  After $-dM_g(Z)$ is processed into stars with the mass $dM_s(Z)$, the metallicity of the gas is in the interval [$Z + dZ$, $Z + 2\,dZ$] ($dM_s = -dM_g$).

Therefore the metallicity distribution of the stars is:

$$\frac{1}{M_s}\frac{dM_s}{dZ} = -\frac{1}{M_{g,0}}\frac{dM_g}{dZ} = \frac{1}{y}\exp\left(-\frac{Z}{y}\right)$$

with $M_s = M_{g,0}$ normalized to 1

- The yield y of metals can be derived from the mean metallicity of the stars:

$$y \simeq 2\,Z_\odot \simeq 0.04$$

which means that the metal production of the bulge was 4% of the mass locked into remnants (higher than in disk?)

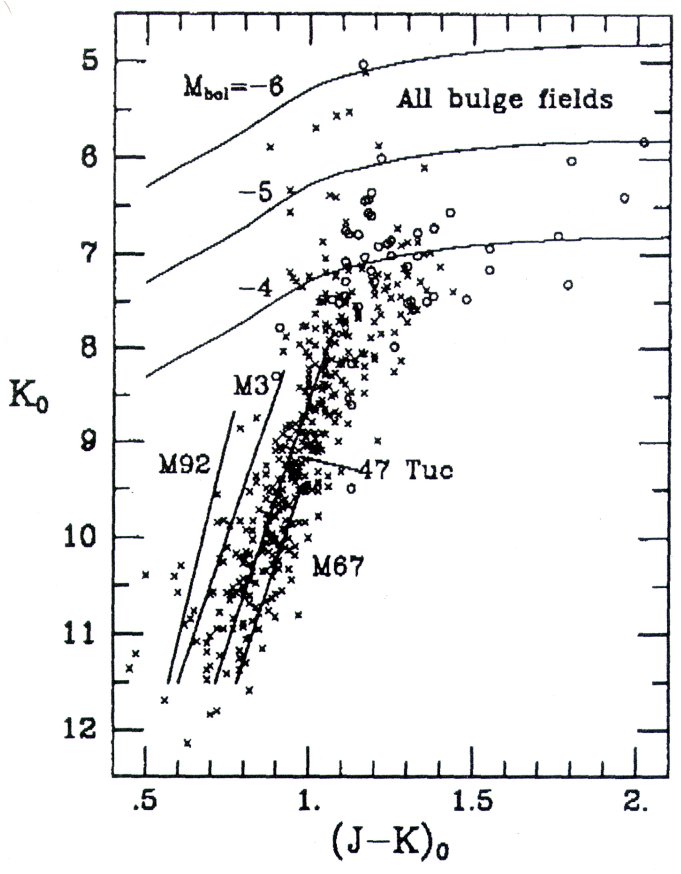

Figure 2: A color-magnitude diagram for all bulge M giants between $b = -3°$ and $-12°$ with data from Papers I and II. Lines of constant M_{bol} are indicated. Solid symbols are the long period variables in the same fields.

The tip of the AGB can be used as age estimator $\Rightarrow$ age > 5 Gyr

see: *ESO/CTIO Workshop on Bulges of Galaxies* (1990)

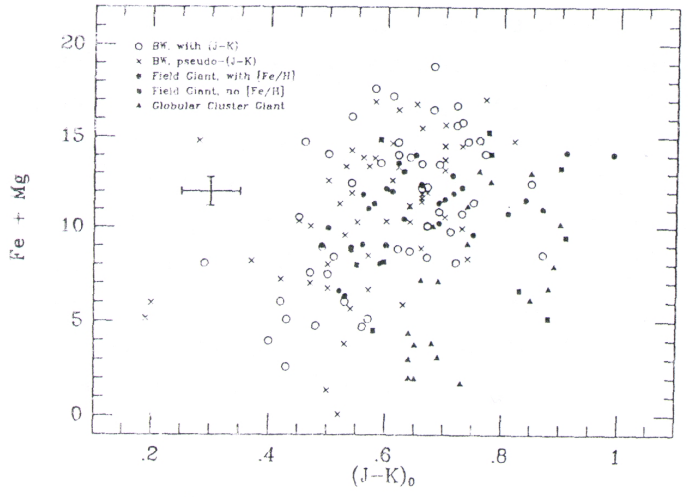

Figure 2: Sum of Fe + Mg line strength (Å) *vs* $(J-K)_o$ colors are dereddened by 0.28 magnitudes. Baade's Window stars are indicated with crosses have infrared colors derived from optical photometry. The filled symbols with the greatest line strength are the most metal rich stars known in the solar neighborhood, as high as [Fe/H] = +0.5 dex. Notice that the Baade's Window stars of the same temperature $(J-K)$ have much greater line strength. Detailed discussion of the measurements is in Rich (1988).

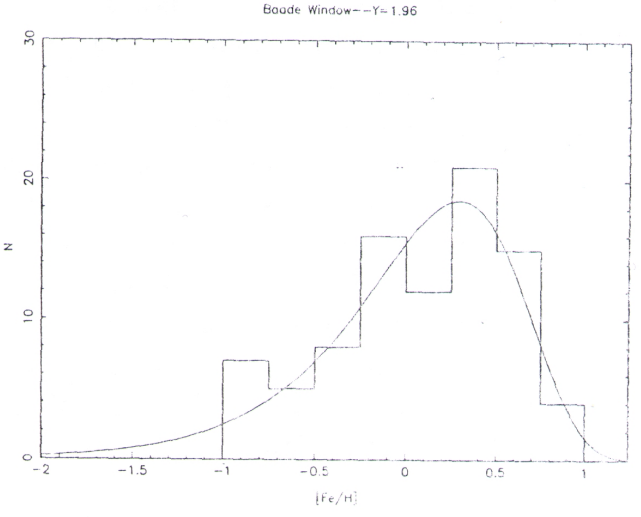

Figure 3: Abundance distribution for 88 K giants in Baade's Window (b=-4°) from Rich (1988). the distribution function is fit with the Simple Model (eqn. 2 in the text) with $y = 1.96 z_\odot = \langle z \rangle$ for Baade's window.

see: *ESO/CTIO Workshop on Bulges of Galaxies* (1990)

5.7 Stellar Population in the Solar Neighbourhood

Two key observations:

- Metallicity-velocity diagram shows 'two' populations:
  $\Rightarrow$ disk-population with $\overline{v_{rot}} \simeq 220\,\frac{km}{s}$ and [Fe/H] $\simeq -1.0... + 0.5$
  $\Rightarrow$ halo-population with $\overline{v_{rot}} \simeq 0\,\frac{km}{s}$ and [Fe/H] $\simeq -0.5... - 3.0$ (like GC!)

- **The metallicity-age diagram for the disk population shows a relatively continuous age distribution between today and** $10 - 13$ **Gyr** (this is consistent with observations of external galaxies, see: Kennicutt).
  The metallicity distribution in the solar neighbourhood is not compatible with a simple closed-box-model: there are not enough metal-poor stars ("G-dwarf problem"). Probable reasons may be pre-enrichment of the disk gas due to bulge formation, radial gas flows or continuous infall of gas.

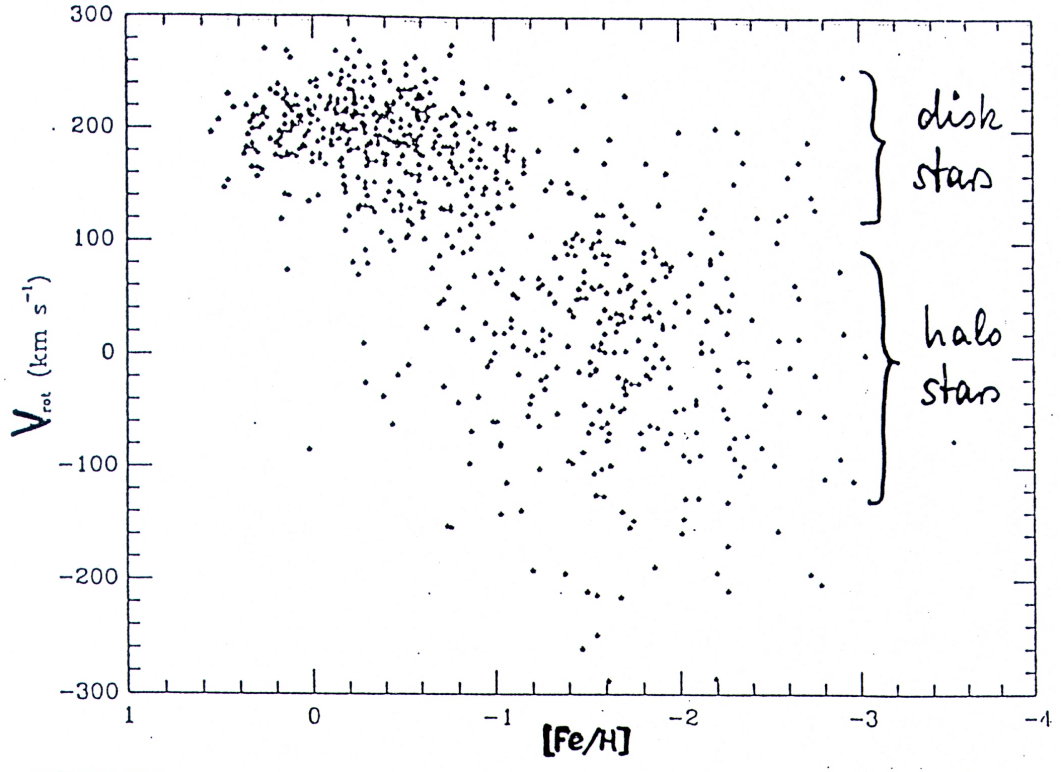

FIGURE 11.3
The relation between rotation velocity relative to the Galactic standard of rest V_{rot} and metallicity, for the sample of proper-motion stars studied by Laird *et al.* (1988). Comparison of this figure with that for the binned data illustrates the difficulty in deducing the reality of a smooth correlation between kinematics and metallicity from data which are averaged into bins, particularly for metallicities near −1 dex.

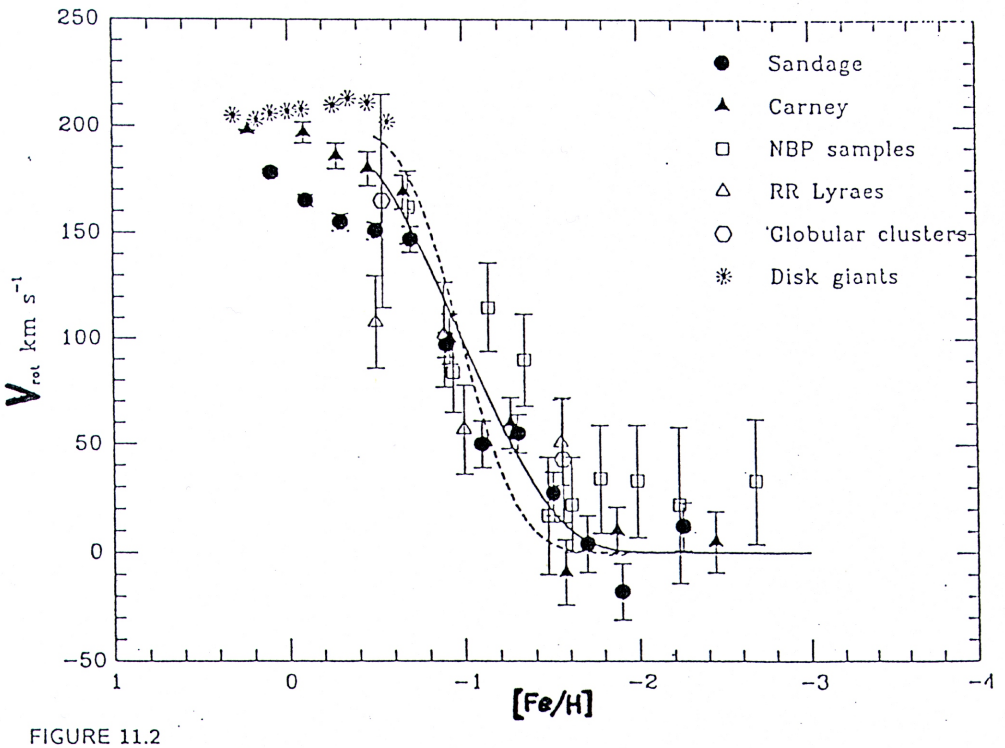

FIGURE 11.2
The relation between rotation velocity relative to the Galactic standard of rest V_{rot} and metallicity, for those samples of field stars with good abundance data discussed in the text. The lines show alternative models, with the solid line being a model involving a smooth correlation between V_{rot} and [Fe/H] over the range $-0.5 \lesssim$ [Fe/H] $\lesssim -1.5$. The dashed line shows a discontinuous relationship between V_{rot} and [Fe/H], with the discontinuity at [Fe/H] $= -1.0$. Both models have been convolved with a Gaussian of dispersion 0.25 dex in metallicity to represent measuring errors.

Element abundances in solar neighbourhood:

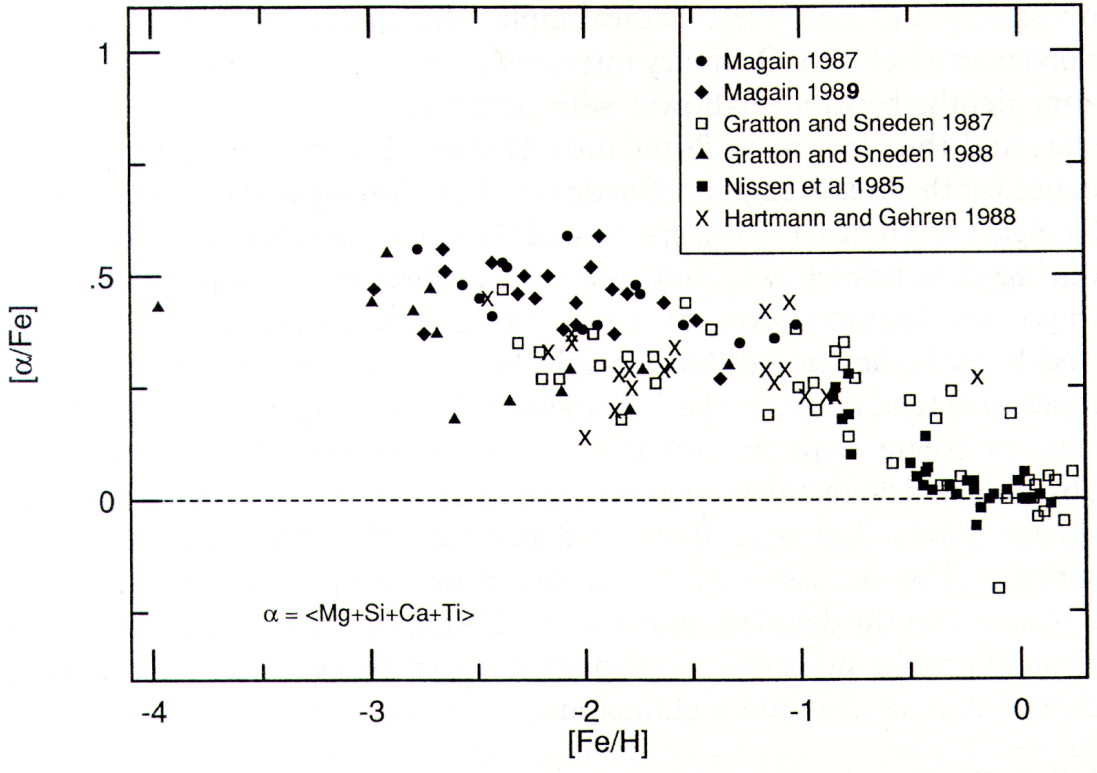

Figure 3 The average α-element abundances as functions of the traditional metallicity indicator Fe. Note that the averaging of the four α-element abundances may blur the possibly real variations with Fe among this group.

see: Wheeler et al. (1989) *ARAA*, **27**

[α/Fe] = logarithmic ratio between mass of α elements (O, Mg, . . .) and Fe mass normalized to the sun:

$$[\alpha/Fe] = \log \frac{\rho_\alpha/\rho_{\alpha_\odot}}{\rho_{Fe}/\rho_{Fe_\odot}}$$

The abundance ratios are correlated with the kinematics of the stars. Stars with little rotation (halo stars) have low metallicity and high α/Fe ratios and therefore have been formed very early when the galaxy was in the early phases of collapse (see SN II vs SN Ia enrichment).

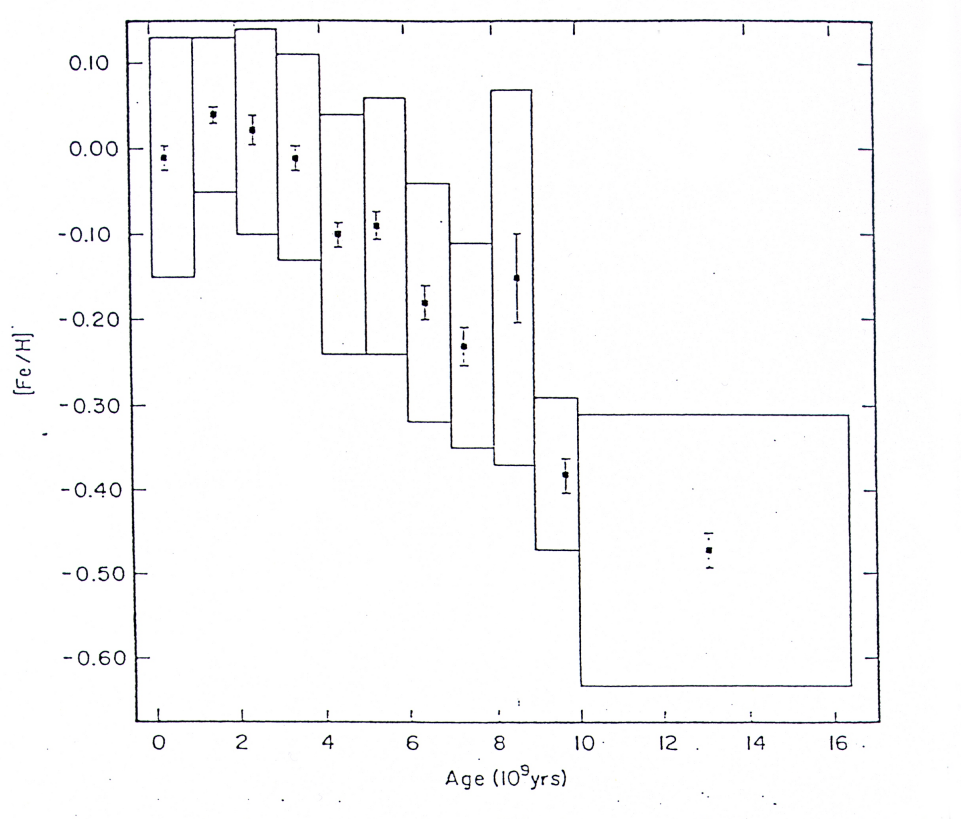

FIGURE 7 The relation between age and metallicity for disk stars in the solar neighborhood (Twarog, 1979). Boxes denote the range of ages referred to by each point, and the $\pm 1\sigma$ spread in [Fe/H] for the age group. Error bars attached to the points denote the standard error in the mean. Note that the mean metallicity increases by a factor of less than four during the lifetime of the disk.

see: Tinsley (1980) *Fundamental of Cosmic Physics*, **5**, 287

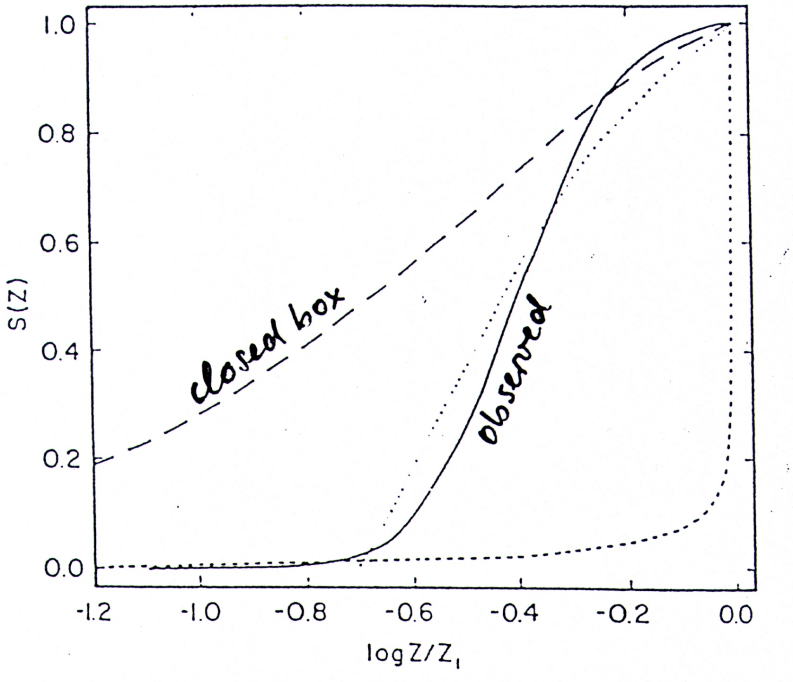

FIGURE 8 Cumulative stellar metallicity distributions. $S(Z)$ is the fraction of stars that have metallicities $\leqslant Z$, with a maximum value Z_1. *Solid line:* log-normal representation of the data for stars in the solar neighborhood; Z_1 is taken as 2 $Z_\odot$ since more metal-rich stars are very rare; $\langle \log Z/Z_\odot \rangle = -0.1$, and $\sigma(\log Z/Z_\odot) = 0.15$, allowing for observational errors (e.g., Pagel, 1979a). *Long dashes:* the "simple" model for chemical evolution (Section 4.2). *Short dashes:* an extreme infall model (Section 4.2.1). *Dots:* a model with a finite initial metallicity (Section 4.2.2).

see: Tinsley (1980) *Fundamental of Cosmic Physics*, **5**, 287

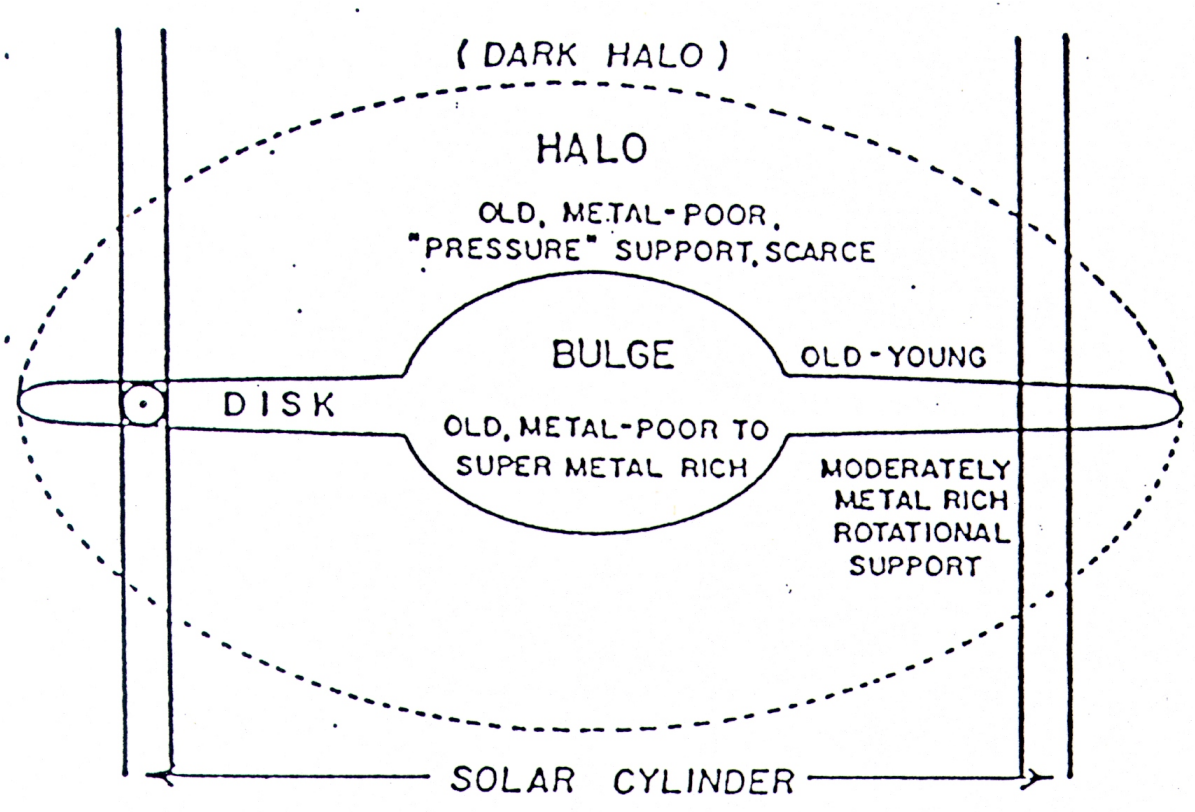

Figure 4: *Schematic cross-sectional view of the Galaxy.*

see: Pagel (1993) *Instituto Astrofisica di Canarias Winter School*

Properties of the Galaxy and the solar cylinder:

	Galaxy	solar cylinder
Age	$10 \text{ to } 15\, Gyrs$	
Mass now in stars	$7 * 10^{10}\, M_\odot$	$45\, M_\odot pc^{-2}$
Mass now in gas	$\approx 7 \cdot 10^{9}\, M_\odot$	$7 \text{ to } 14\, M_\odot pc^{-2}$
Gas fraction	0.1	$0.14 \text{ to } 0.25$
Surface brightness		$23\, m_V$, $m_{bol}\ arcsec^{-2}$
$(M/L_V)\,/\,(M/L_V)_\odot$	5	3
Processes tending to deplete the gas:		
Average past SFR	$(5-7)\,\alpha^{-1}\, M_\odot yr^{-1}$	$(3-4.5)\,\alpha^{-1}\, M_\odot pc^{-2} Gyr^{-1}$
Gas consumption time	$\approx 1\, Gyr$	$1.5 \text{ to } 5\, Gyr$
Processes tending to restore the gas:		
Mass ej. from AGB + PN		$0.8\, M_\odot pc^{-2} Gyr^{-1}$
Mass ej. from O stars		$\approx 0.05\, M_\odot pc^{-2} Gyr^{-1}$
Mass ej. from SN	$\approx 0.15\, M_\odot yr^{-1}$	$\approx 0.05\, M_\odot pc^{-2} Gyr^{-1}$
(Total mass ejection from stars		$\approx 1\, M_\odot pc^{-2} Gyr^{-1}$)
Net inflow from IGM	$\leq 2\, M_\odot yr^{-1}$	$\leq 1\, M_\odot pc^{-2} Gyr^{-1}$

see: Pagel (1993) *Instituto Astrofisica di Canarias Winter School*

Classical interpretation of these data by Eggen, Lynden-Bell and Sandage:
(see: (1962) *ApJ*, **136**, 748)

The Galaxy was built in two phases:

1. In the beginning the gas collapsed within a few hundred million years from a large volume:
   → metal poor stars (and GCs) with negligible rotation → **halo**
2. After that a slower, dissipative phase followed:
   → because of its angular momentum, the gas concentrated more and more in the **disk** (it may have been pre-enriched with metals expelled during bulge-formation).
   → stars formed in the disk due to instabilities and triggering by the continuous infall of gas.

This model is very likely to be too simple but correct in essence!

The modern view is that galaxies form via **hierarchical clustering.**
(see, e.g., discussion in Norris, J. (1987) in *The Galaxy*,
or Katz, N. (1992) *ApJ*, **391**, 502)